Upconversion Luminescent Chemodosimeter Based on NIR Organic Dye for Monitoring Methylmercury In Vivo

Huiran Yang, Chunmiao Han, Xingjun Zhu, Yi Liu, Kenneth Yin Zhang, Shujuan Liu, Qiang Zhao, Fuyou Li,* and Wei Huang**

While most luminescent organic dyes display intense Stokes fluorescence, some of them exhibit unique single-photon frequency upconversion luminescence (FUCL). Compared to conventional anti-Stokes luminescence of lanthanides and two-photon excitation, FUCL materials display adjustable spectrum area and require a much lower excitation power. Although this is very beneficial for biological applications in the perspective of reducing photodamage to biological samples and photobleaching of the dyes, the utilization of FUCL for biosensing and bioimaging in vivo has not been reported. In this study, we developed a near-infrared (NIR) rhodamine derivative (FUC-1) as a chemodosimeter, which displays weak luminescence but undergoes thiolactone ring-open process leading to luminescence turn-on in response to mercury(II) cation or methylmercury with good selectivity and high sensitivity in aqueous solution. Interestingly, FUC-1 displays particular FUCL, excitation at 808 nm leads to luminescence at 745 nm. Compared to Stokes luminescence resulted from excitation at 630 nm, the use of FUCL lowers the detection limit of Hg^{2+} to be 0.207 nM. FUC-1 has been used for FUCL bioimaging of methylmercury in live cells and mice. To the best of our knowledge, this is the first example of FUCL biosensing and bioimaging in vivo using visible and NIR fluorescence of small-molecular dyes.

1. Introduction

Mercury is one of the most hazardous and ubiquitous heavy metals, which may accumulate in human body through the food chain.[1] It shows high permeability into skin, respiratory and gastrointestinal systems of the human body, and can cause serious damage to the central nervous system.[2] Therefore, it is very important to develop various methods to efficiently detect mercury in vitro and in vivo. Luminescence bioimaging provides an important means of visualizing morphological details of tissues with subcellular resolution and has become a powerful tool for manipulation in the biological analysis and medical diagnosis and treatment.[3] Although a large number of mercury-sensitive luminescent probes have been reported, which include fluorescent dyes,[4] phosphorescent transition-metal complexes,[5] and nanoparticles,[6] most of them are only used for monitoring inorganic mercury(II) cation, not applicable for sensing methylmercury ($MeHg^+$).[7] As an organic form of mercury, $MeHg^+$ causes much higher biotoxicity to living organisms compared to inorganic mercury, because it is a liposoluble and bioaccumulative toxicant that shows very high affinity for thiol groups on cysteine and cysteine-containing proteins, and hence detection and monitoring of $MeHg^+$ are of particular importance.

During biosensing and bioimaging in living animals, low-energy excitation using the near-infrared (NIR) light is preferred since it avoids photobleaching of dyes and photodamage to animals, reduces autofluorescence, deepens penetration depth, and improves signal-to-noise ratio (SNR) compared to the UV and visible light excitation.[8] And the design and synthesis of new NIR organic probes for $MeHg^+$ possess great importance and promising applications.

Upconversion luminescent (UCL) materials commonly including lanthanide-doped upconversion nanoparticles (UCNPs) and two-photon absorption materials, which are excitable by long-wavelength light and emit short-wavelength light. UCL materials have been widely used in biological application due to their unique properties, such as large anti-Stokes shift, limited autofluorescence from biological samples, and

H. R. Yang, Dr. K. Y. Zhang, Prof. S. J. Liu, Prof. Q. Zhao, Prof. W. Huang
Key Laboratory for Organic Electronics and Information Displays and Institute of Advanced Materials (IAM)
Jiangsu National Synergetic Innovation Center for Advanced Materials (SICAM)
Nanjing University of Posts and Telecommunications (NUPT)
Nanjing 210023, P. R. China
E-mail: iamqzhao@njupt.edu.cn; wei-huang@njtech.edu.cn
H. R. Yang, Dr. C. M. Han, X. J. Zhu, Dr. Y. Liu, Prof. F. Y. Li
Department of Chemistry
Fudan University
Shangha 200433, P. R. China
E-mail: fyli@fudan.edu.cn
Prof. W. Huang
Key Laboratory of Flexible Electronics (KLOFE) and Institute of Advanced Materials (IAM)
Jiangsu National Synergetic Innovation Center for Advanced Materials (SICAM)
Nanjing Tech University (NanjingTech)
Nanjing 211816, P. R. China

DOI: 10.1002/adfm.201504501

high SNR.[9,10] Recently, Li et al. have first demonstrated biosensing and bioimaging of $MeHg^+$ in small animals using a sensory nanosystem for $MeHg^+$ based on luminescence resonance energy transfer between lanthanide UCNPs and organic dyes.[11] Organic compounds that exhibit frequency upconversion luminescence (FUCL) are another family of luminescent dyes that convert low-energy excitation to high-energy emission.[12] While Stokes luminescence occurs after excitation of the dye from the zero point vibrational level of the ground electronic state (S_0) to the first excited electronic state, FUCL begins with excitation of the dye at thermally excited vibrational–rotational energy levels of ground electronic state (S_t) to the first excited electronic state in consequence of the continuous optical pumping, accompanying with the fluorescence into lower sublevels of the ground electronic state (**Figure 1**).[13] Compared to UCNPs, the signaling units of FUCL are single-molecular organic dyes, which show higher absorptivity and tunable excitation and emission wavelengths, but reduced photostability. To date, limited examples of FUCL organic dyes have been reported,[14] and none has been applied for UCL sensing and bioimaging in small animals.

In this work, we designed and synthesized an NIR chemodosimeter FUC-1, bearing a monothiospirolactone group in the rhodamine architecture. Due to the strong binding between mercury and sulfur atoms, FUC-1 underwent unique transformation from the nonfluorescent thiolactone form to the NIR fluorescent ring-opening form. FUC-1 exhibits high selectivity and sensitivity toward both mercury(II) cation and methylmercury. Meanwhile, FUC-1 exhibits anti-Stokes FUCL, which occurs at 745 nm in the NIR region upon photoexcitation at 808 nm. The utilization of FUC-1 in luminescence bioimaging for mercury ex vivo and in vivo has been demonstrated. The results indicate a prominent signal-to-noise ratio and deep tissue penetration in upconversion bioimaging mode.

2. Results and Discussion

2.1. Synthesis and Characterizations

The probe FUC-1 was obtained by "one pot synthesis" from a precursor ND-1 (**Scheme 1** and Figure S1, Supporting Information).[15] ND-1 was mixed with phosphorus oxychloride to obtain chloride derivatives (FUC-Cl) of ND-1. Without purification, FUC-Cl was stirred in saturated Na_2S aqueous solution for 12 h, and the crude product obtained was chromatographed on silica eluting with ethyl acetate and petroleum ether (1:10, v:v) to afford FUC-1 in 57% yield as yellow powder.[16] FUC-1 and ND-1 were characterized by ^1H NMR, ^{13}C NMR, and MALDI-TOF MS spectra (Figures S13–S18, Supporting Information).

2.2. Photophysical Properties

As an NIR organic dye, ND-1 exhibits remarkable NIR absorption and emission with high fluorescence quantum yields (Figure S1, Supporting Information). In ethanol, ND-1 exhibits a sharp absorption band at 710 nm with the molar absorption coefficient (ε) of 101700 M^{-1} cm^{-1} and the emission maximum occurs at 745 nm. The absolute Stokes and FUCL quantum yields (Φ) are measured to be 26.5% and 9.8%, respectively, in $CHCl_3$ (Table S1, Supporting Information). FUC-1 did not exhibit the absorption or fluorescence peak in the NIR region due to its thiolactone type. The thiolactone ring-open process was not disturbed in physiological pH range (pH 5–10) (Figure S3, Supporting Information). These spectral difference in the NIR area indicated that FUC-1 can be used as an organic probe due to the thiolactone ring-open process induced by mercury (Scheme 1 and Figure S1, Supporting Information).

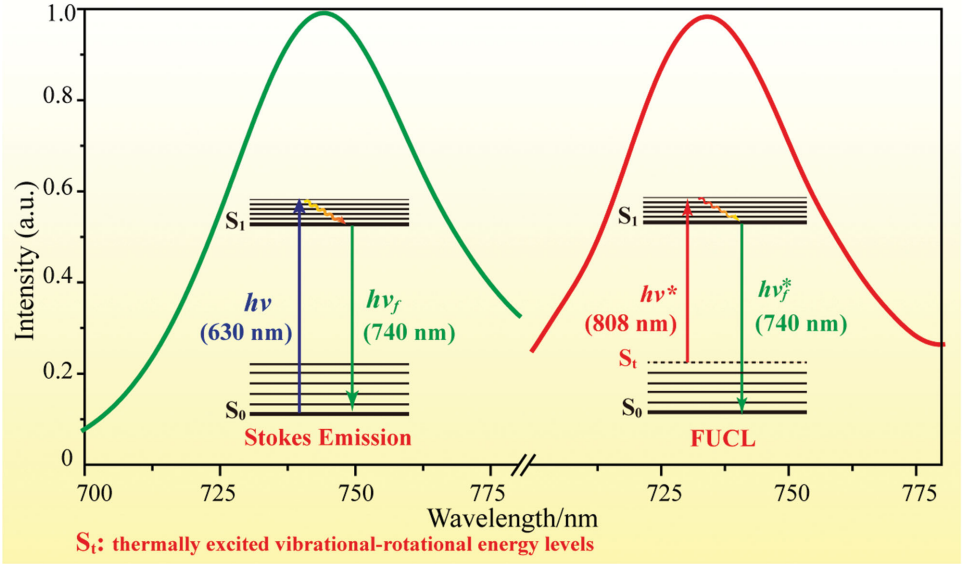

Figure 1. The mechanism of Stokes luminescence emission and anti-Stokes frequency upconversion luminescence emission. In Stokes emission (left), the optical excitation from the zero point vibrational level of the ground electronic state (S_0) to the first excited electronic state (S_1) and a subsequent radiative decay to the ground state. In the FUCL (right), the optical excitation from the thermally excited vibrational–rotational energy levels of ground electronic state (S_t) to the first excited electronic state (S_1), accompanying with the high-energy luminescence into lower sublevels of the ground state.

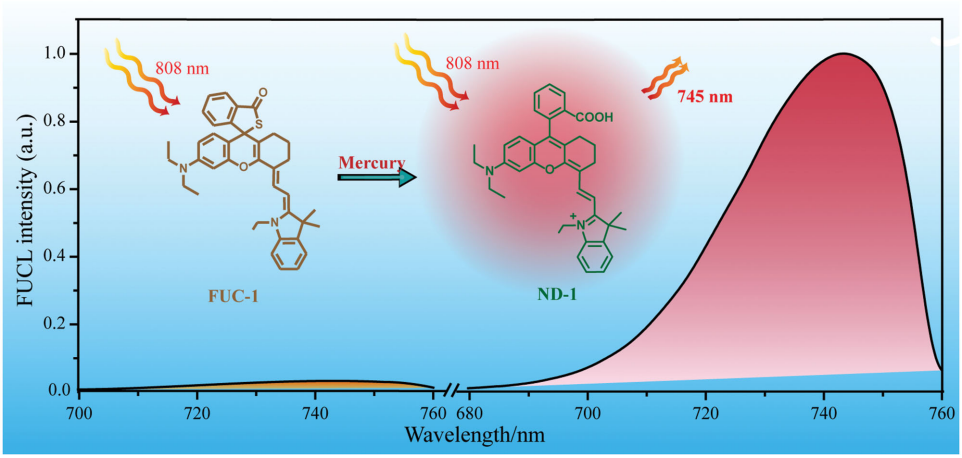

Scheme 1. The diagram for FUC-1 to monitor mercury by using the frequency upconversion luminescence emission.

Although some rhodamine derivatives with cyclic thiolactones have been reported for mercury detection,[4a,16,17] FUC-1 displays both excitation and emission in the NIR region, which facilitates its application in in vivo imaging with minimized autofluorescence interference and improved penetration depth. More importantly, ND-1 exhibits the anti-Stokes FUCL, which further lowers the detection limit of mercury and improves the SNR of in vivo imaging (vide infra). In this work, ND-1 displays a short-wavelength luminescence at 745 nm upon excitation at 808 nm (Scheme 1). The anti-Stokes emission spectrum matches well with that obtained under excitation at 710 nm. In the FUCL process, the thermal vibration levels of ND-1 provide the insufficient energy to excite ND-1 from the ground electronic state to the first excited electronic state and a subsequent radiative decay to the ground state, accompanying with a high-energy luminescence emission, which is the same as the Stokes emission.

2.3. Absorption and Stokes Emission Response of FUC-1 to Mercury

As mentioned before, FUC-1 has its unique potential to monitor mercury ex vivo and in vivo. Firstly, the spectrum measurement was carried out to verify the ability of mercury detection. The absorption and fluorescence titration of Hg^{2+} to FUC-1 (10 μM) were conducted in HEPES buffer/ethanol (v/v, 1:1) solution. As shown in **Figure 2**a, the absorption titration spectra show a remarkable hyperchromic shift at 710 nm, leading to a solution color change from colorless to light green (Figure S7, Supporting Information). Hence, FUC-1 would be a practical "naked-eye" probe for Hg^{2+} in aqueous solutions. Meanwhile, the absorbance at 710 nm was linearly related to the concentration of additive Hg^{2+}. Using the absorption measurement, we could quantitatively detect mercury ions in the sample with high accuracy. In the fluorescence titration, with addition of Hg^{2+}, an obvious change of the fluorescence spectra was observed. As shown in Figure 2c, under excitation at 630 nm, fluorescence at 745 nm was turned on with a linear relationship between the emission intensity and the additive Hg^{2+} within 0–3 μM. Pure FUC-1 displayed no absorption and fluorescence in the NIR region due to its thiolactone structure. The unique structural transformation to open-ring form induced by Hg^{2+} was accompanied with the absorption and fluorescence increase in the spectrum.

The use of FUC-1 to monitor $MeHg^{+}$ in aqueous solutions has also been demonstrated. As shown in Figure 2, with the addition of $MeHg^{+}$, obvious changes were observed in both absorption and fluorescent spectra. Similar response of the absorption peak at 710 nm and the fluorescent peak at 745 nm was observed as that in the Hg^{2+} titration. But the reaction process between FUC-1 and $MeHg^{+}$ is different from that of Hg^{2+}. The absorption at 710 nm and the fluorescent intensity at 745 nm change a little with the addition of 0–1 equiv. $MeHg^{+}$. With the continuous addition of $MeHg^{+}$, the remarkable enhancement is observed in both absorption and fluorescent spectra. These results indicated that the unique structural transformation to open-ring form can be induced by both $MeHg^{+}$ and Hg^{2+}, and FUC-1 exhibits its ability to monitor both $MeHg^{+}$ and Hg^{2+} in aqueous solution.

2.4. Responsive Mechanism of FUC-1 to Mercury

In the above discussion, FUC-1 displays a linear spectral response to Hg^{2+}, but the response to $MeHg^{+}$ is uneven. This indicates that the reaction mechanism of FUC-1 with $MeHg^{+}$ and Hg^{2+} is different. The reaction mechanism between FUC-1 and Hg^{2+} was proposed to be coordination binding of two FUC-1 molecules to the same Hg^{2+} due to the sulfophile affinity of mercury (**Scheme 2**). It was supported by Job's plots, which determined the optimal ratio of chemometric number between FUC-1 and Hg^{2+} to be 2:1 (Scheme 2c). After desulfurization and hydrolysis reaction, FUC-1 was changed to ND-1 finally. This mechanism was supported by the MALDI-TOF MS analysis. In addition to the signal at m/z 588.2 corresponding to FUC-1, another peak signal at m/z 571.2 corresponding to ND-1 was observed in the presence of Hg^{2+} (Scheme 2b). Additionally, the ^{1}H NMR spectra (Figure S4a, Supporting Information) indicated the transformation from FUC-1 to ND-1

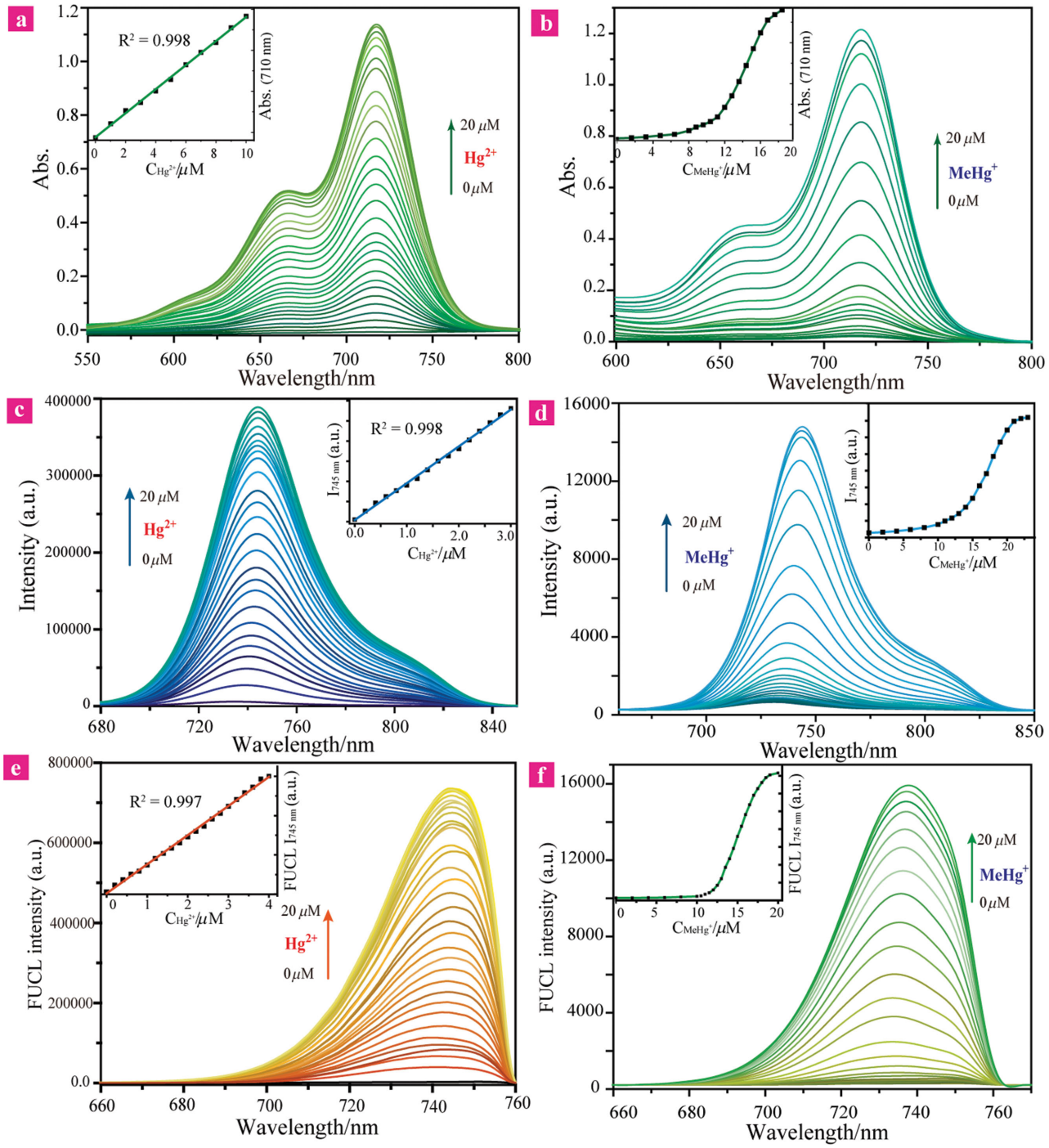

Figure 2. Optical response of FUC-1 to mercury. a, b) Changes of the absorption of FUC-1 (10 μM) in HEPES buffer/ethanol (v:v, 1:1) solution with addition of different amounts of Hg^{2+} or $MeHg^{+}$ (0–2 equiv.), respectively. Inset: the absorption of FUC-1 at 710 nm with addition of different amounts of Hg^{2+} or $MeHg^{+}$. c, d) Fluorescence spectra (excitation at 630 nm) of FUC-1 (10 μM) in HEPES buffer/ethanol (v:v, 1:1) solution with the addition of Hg^{2+} or $MeHg^{+}$ (0–20 μM). Inset: the luminescence intensity of FUC-1 at 745 nm with addition of different amounts of Hg^{2+} or $MeHg^{+}$. e, f) FUCL emission spectra of FUC-1 (10 μM) in HEPES buffer/ethanol (v:v, 1:1) solution upon addition of Hg^{2+} or $MeHg^{+}$ within the range 0–20 μM, respectively. Under illumination with an 808 nm laser, collocating with a 775 nm short-pass filter.

after completely reacting with Hg^{2+}. FUC-1 reacts with $MeHg^{+}$ in a different manner (Scheme 2). With addition of 0–1 equiv. $MeHg^{+}$, FUC-1 reacts with $MeHg^{+}$ forming a stable intermediate (FUC-1-$MeHg^{+}$). With the continuous addition of $MeHg^{+}$, the subsequent intermediate was unstable and transformed to ND-1 after the desulfurization and hydrolysis reaction. This mechanism has been demonstrated by the MALDI-TOF MS spectra (Figure S5, Supporting Information). In the absence of

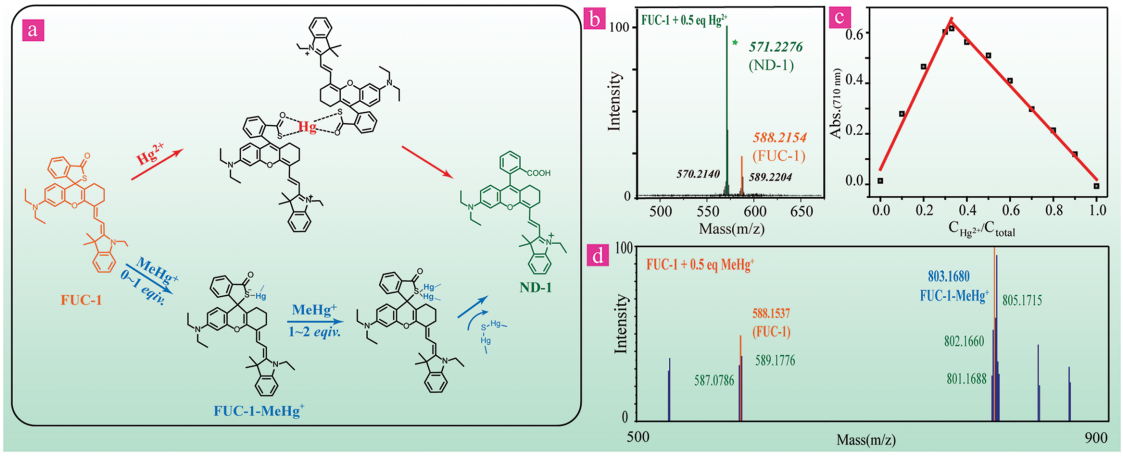

Scheme 2. The proposed sensing mechanism and main evidences of FUC-1 to both Hg^{2+} and $MeHg^{+}$. a) The proposed sensing mechanism of FUC-1 to both Hg^{2+} and $MeHg^{+}$. b) The MALDI-TOF MS spectrum of FUC-1 under 0.5 equiv. Hg^{2+}. c) Job's plot of the complex between FUC-1 and Hg^{2+} in HEPES buffer/ethanol (v:v, 1:1) solution. Total concentration of FUC-1 and Hg^{2+} was kept constant at 100 μM. d) MALDI-TOF MS spectrum of FUC-1 with 0.5 equiv. $MeHg^{+}$.

$MeHg^{+}$, the m/z peak at 588.2 refered to FUC-1; a new peak at 803.2 was observed in the presence of 0.5 equiv. $MeHg^{+}$, which refered to the intermedicate FUC-1-$MeHg^{+}$; an m/z peak at 573.2 appeared with the addition of 1.5 equiv. $MeHg^{+}$, which indicated that FUC-1 was transformed to ND-1 finally.

2.5. Upconversion Luminescence Response of FUC-1 to Mercury

Interestingly, the open-ring form of FUC-1 showed anti-Stokes frequency upconversion luminescence, and excitation using a long wavelength light source led to short wavelength fluorescence. Therefore, we evaluated the sensing performance of FUC-1 to both Hg^{2+} ions and $MeHg^{+}$ using the FUCL emission spectra. Using an 808 nm laser as the excitation source, collocating with a 775 nm short-pass filter, an intense FUCL emission band at 745 nm was observed upon the addition of Hg^{2+}. Likewise, a linear relationship between the FUCL emission intensity and the additive concentration of Hg^{2+} (0–4 μM) was observed (Figure 1e). Meanwhile, similar results were observed in the $MeHg^{+}$ titration, and the responsive process was attributed to the mechanism that we described above.

On this basis, we attempt to verify the detection sensitivity of FUC-1 to Hg^{2+} by both Stokes luminescence and anti-Stokes upconversion luminescence methods. The Environmental Protection Agency (EPA) standard for the maximum allowable level of Hg^{2+} in drinking water is 2 ppb.[18] To take this chemodosimeter in practical use, it is necessary to test the limit of detection (LOD) for Hg^{2+}. By using the ordinary Stokes emission titration, we found that the LOD for Hg^{2+} is 2.78 nM (0.55 ppb), which can be reduced to approximately 0.207 nM (0.041 ppb) by using the FUCL. This is because the instrumental error (σ) was minimized when using FUCL. Therefore, we could find that FUC-1 has an excellent sensitivity and accuracy for detecting mercury in aqueous solution by both Stokes emission and anti-Stokes emission measurements.

To test the selectivity of FUC-1 toward mercury in the presence of other metal ions, we measured both the Stokes luminescence and FUCL emission spectra of FUC-1 in the presence or absence of different metal ions, including alkali metals ions, alkali-earth metals ions, and transition-metal ions in HEPES buffer/ethanol (v:v, 1:1) solutions. As shown in **Figure 3**b, no obvious FUCL enhancement was observed in the presence of other metals ions except Ag^{+} and Au^{+}. Ag^{+} and Au^{+} are soft acid with the ability of reaction with the sulfur atom like mercury.[19] However, the FUCL enhancement induced by Ag^{+} and Au^{+} is not as significant as that induced by Hg^{2+} and $MeHg^{+}$. Meanwhile, we carried out the same measurement using the Stokes luminescence spectra (Figure 3a). The same results were obtained. All these results confirmed that FUC-1 has good selectivity to Hg^{2+} and $MeHg^{+}$ against other metal ions via both Stokes luminescence and FUCL.

2.6. Monitoring Mercury in Living Cells

Before using FUC-1 to imaging intracellular mercury, we employed methyl thiazolyl tetrazolium (MTT) assay to investigate the cytotoxicity of ND-1 and FUC-1 (Figure S9, Supporting Information). The cell viability sustained 90%–100% upon ND-1 or FUC-1 treatment for 24 h, which indicated that these two dyes did not affect the cell viability evidently. This laid the groundwork for the further application of FUC-1 in sensing mercury ex vivo and in vivo.

In a typical experiment of intracellular imaging, Hela cells were incubated with 0.1 and 1.0 μM $MeHg^{+}$ for 30 min, while the cells without $MeHg^{+}$ treatment was used as control. After washing with PBS buffer for three times, all the cells were incubated with FUC-1 (5 μM) for 30 min. Then these cells were used for confocal laser-scanning luminescence microscopy experiments. Upon excitation with 630 nm laser, the Stokes emission was collected at 700–760 nm. With a thiolactone structure FUC-1 shows no emission in cells (**Figure 4**). In the presence of $MeHg^{+}$, due to the structural transformation from thiolactone to the open-ring form, weak emission was detected in the cells incubated with 0.1 μM (20 ppb) $MeHg^{+}$, and much

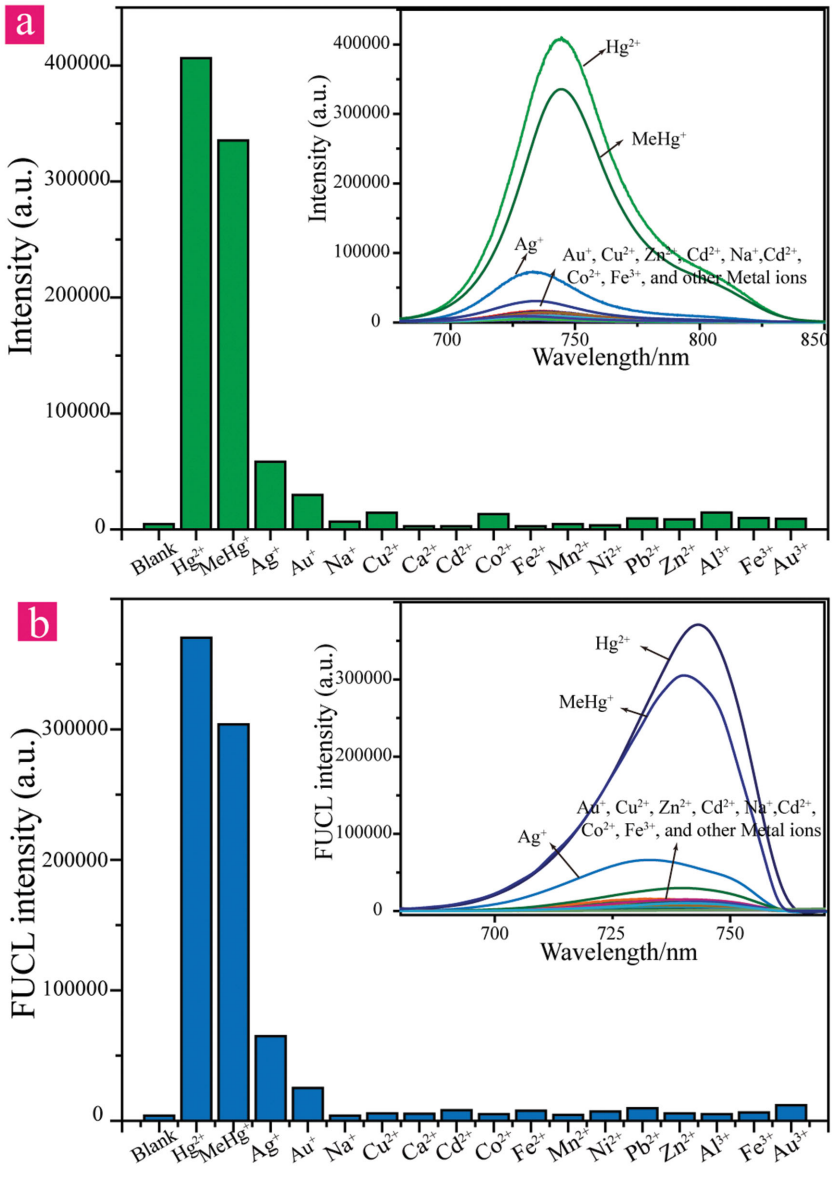

Figure 3. Selectivity of the probe FUC-1 for Hg^{2+} and $MeHg^{+}$ in HEPES buffer/ethanol (v:v, 1:1) solution via both Stokes luminescence and FUCL signals. a) Green bars indicate the fluorescence enhancement at 730 nm with addition of 1 equiv. metal ions. Inset: luminescence spectra of FUC-1 with addition of 1 equiv. metal ions (excitation at 650 nm). b) Blue bars indicate the FUCL enhancement at 730 nm with addition of 1 equiv. metal ions. Inset: FUCL spectra of FUC-1 with addition of 1 equiv. metal ions (excitation at 808 nm). Metal ions: blank, Hg^{2+}, Na^{+}, Au^{+}, Ag^{+}, Cu^{2+}, Ca^{2+}, Zn^{2+}, Fe^{2+}, Mn^{2+}, Ni^{2+}, Pb^{2+}, Cd^{2+}, Co^{2+}, Al^{3+}, Fe^{3+}, and Au^{3+}.

stronger signal was collected from the cells treated with 1.0 μM (200 ppb) $MeHg^{+}$ (Figure S10, Supporting Information). This indicated that FUC-1 could monitor $MeHg^{+}$ in living cells.

To prove the ability of FUC-1 in monitoring intracellular $MeHg^{+}$ using the FUCL, laser-scanning upconversion luminescence microscopy (LSUCLM) experiments were carried out. Using a continuous-wave 808 nm laser as the excitation source, we collected FUCL emission at 700–760 nm as the detection signals. The experimental condition was the same as that of the Stokes luminescence imaging. Incubating Hela cells with 5 μM FUC-1 for 30 min without adding $MeHg^{+}$, almost no FUCL signals was observed. The luminescence intensity analysis in living cells was shown in Figure S11 in the Supporting Information, and the obviously enhanced FUCL signals were detected when the cells were pretreated with $MeHg^{+}$. All these results verified powerfully that FUC-1 could monitor $MeHg^{+}$ ions in living cells using either NIR Stokes emission or FUCL as detection signals.

2.7. Monitoring Mercury In Vivo

Methylmercury, as an organic form of mercury, can enter the aquatic food chain to become the predominant dietary source of mercury in humans.[20] It is very toxic as it passes the blood brain barries owing to its lipid solubility. A remarkable characteristic of methylmercury poisoning is the selective damage to the central nervous system and the developing brain. In the work aforementioned, we found that FUC-1 could monitor $MeHg^{+}$ in living cells. Hence, we attemp to verify FUC-1 as a luminescent probe to monitor trace $MeHg^{+}$ in living animals. The in vivo imaging is performed with a modified upconversion luminescence in vivo imaging system designed by our group. Two external adjustable lasers at 670 and 808 nm and an Andor DU897 EMCCD were used as the excitation source and the signal collector, respectively.

For ordinary small animal imaging, we use a continuous-wave laser at 670 nm (power density ≈ 8.5 mW cm^{-2}) as the excitation source, collecting the luminescence between 695 and 770 nm as the detection signals (**Figure 5**). The experimental group mouse was injected intravenously (i.v.) with 0.17 mg wt^{-1} kg $MeHg^{+}$ for 5 h and then injected (i.v.) with 0.20 mL FUC-1 (50 μM). Obvious Stokes luminescence signal can be detected, and most of the signals were concentrated in the abdominal cavity area of the mouse. Meanwhile, only very weak luminescence signal can be detected for the control mouse which was not injected with $MeHg^{+}$. Compared to the control group, the luminescence intensity in the $MeHg^{+}$-pretreatment group increased more than fivefold. A World Health Organization (WHO) report concluded that the lowest effect level or levels of mercury associated with a low risk (about 5%) was about 10–40 ppb in blood for humans. The usage amount of $MeHg^{+}$ in the bioimaging process is 4.31 ppb (0.02 μM), which is below the minimum standard provided by WHO. Besides, the SNR was another important indicator of bioimaging capability and was determined using the following formula: SNR = $(I_{ROI1}-I_{ROI3})/(I_{ROI2}-I_{ROI3})$, where I_{ROI1}, I_{ROI2}, and

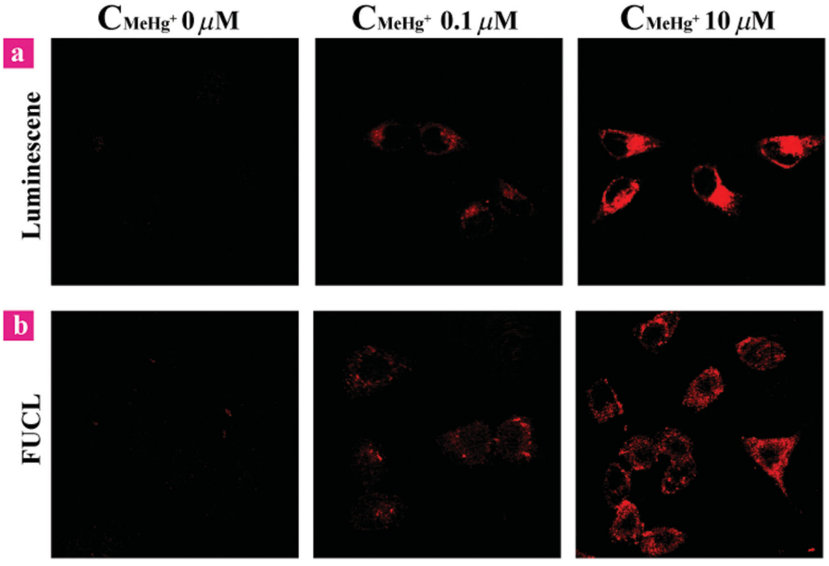

Figure 4. Confocal luminescence imaging of living Hela cell lines. a) Luminescence and b) upconversion luminescence imaging of Hela cells incubated with FUC-1 (10 μM) to montior $MeHg^+$. These three columns indicated that the Hela cells were incubated with 0, 0.1 μM (20 ppb), and 10 μM $MeHg^+$, from left to right. The luminescence and FUCL images were all collected at 700–760 nm, using 635 and 808 nm laser as the excitation source, respectively.

I_{ROI3} represented the luminescence intensity of the signal area, the noise area, and the background area, respectively. The SNR of FUC-1 in monitoring $MeHg^+$ was calculated to be 3.16 by using its outstanding NIR luminescence property. All these results indicated that FUC-1 exhibits good capability of detecting trace amount of $MeHg^+$ in vivo using its excellent NIR emission.

Using a continuous-wave laser at 808 nm as the excitation source, collecting the same range of luminescence as the detection signals, we obtained the upconversion luminescence living animal images to monitor $MeHg^+$ in vivo. The power density on the surface of nude mouse was 55 mW cm^{-2}, which was much lower than that used in two-photon excited bioimaging and UCNPs bioimaging. The $MeHg^+$-pretreatment mouse was also injected (i.v.) with 0.17 mg wt^{-1} kg $MeHg^+$ for 5 h and then injected (i.v.) with 0.20 mL FUC-1 (50 μM) before the bioimaging. Very weak FUCL emission at the abdomen was detected in the mouse injected with normal saline and FUC-1 (Figure 5), while the FUCL signals in the experimental mouse injected with $MeHg^+$ and FUC-1 were fourfold stronger than that of the control animal. Furthermore, the SNR of FUCL bioimaging is 3.48, which was slightly improved compared to the SNR of fluorescence bioimaging (3.16), because the autofluorescence in the sample was reduced. These results indicated that FUC-1 can also detect trace amount of mercury in vivo by using its unique FUCL property.

As shown in **Figure 6**, compared to the control group, both the Stokes emission signals and the FUCL signals were increased obviously in the $MeHg^+$-pretreatment group, especially in the liver and kindeys. From the bloodstream, $MeHg^+$ can be taken up by all tissues and accumulated mainly in kidneys and liver for animals. So we could find both the Stokes emission and the FUCL emission signals distributed in liver and kindeys (Figure 6). Excretion of $MeHg^+$ occurs mainly via the feces and urine, which respectively represent the source of liver and kidneys.[21] All these were observed via the bioimaging results. The signals in heart indicated the transport through the blood, whiles the signals in intestines, liver, and kindeys are due to the absorption and excretion through the digestive system. These bioimaging results indicated that FUC-1 could monitor the distribution and metabolism of mercury in vivo using its outstanding NIR emission and FUCL properties.

3. Conclusion

In summary, we have constructed an NIR upconversion luminescent $MeHg^+$ chemodosimeter FUC-1 based on frequency upconversion luminescence mechanism by a design strategy of using the thiospirolactone interactions between Hg and S. FUC-1 exhibited the amazing FUCL, excellent NIR fluorescence enhancement, high selectivity, and low limit of detection for mercury. Furthermore, we can use this FUCL probe FUC-1 for monitoring mercury ex vivo and in vivo by both Stokes luminescence and upconversion luminescence bioimaging. To the best of our knowledge, this is the first example of FUCL biosensing and small-animal bioimaging based on small-molecule organic dyes. The design strategy for FUCL-based probes in this work is not limited to mercury sensing; the incorporation of other responsive moiety into FUCL dyes will lead to a new generation of probes for specific analytes for promising application in biosensing and bioimaging in vitro and in vivo.

4. Experimental Section

Synthesis of ND-1: Compound **1** (6-(*N*,*N*-diethylamino)-9-(2-carboxyphenyl)-1,2,3,4-tetrahydroxanth-ylium perchlorate, 0.5 mmol), compound **2** (2-(2-anilinovinyl)-1-ethyl-3,3-dimethyl-3H-indolium iodide, 0.55 mmol), and KOAc (0.05 mmol) were added into a flask and dissolved with 15 mL acetic anhydride, and then stirred at 50 °C for 2 h. This reaction was quenched with 10 mL H_2O, then the solvent was removed and the product was purified with silica chromatography using CH_2Cl_2 to CH_2Cl_2/methanol (100:1 to 10:1) as eluent. Yield 310 mg (54%). ^{1}H NMR (400 MHz, CD_3OD) δ = 8.65 (d, J = 14.1 Hz, 1H), 8.09 (dd, J = 7.6, 1.3 Hz, 1H), 7.60 (m, 2H), 7.52 (d, J = 7.0 Hz, 1H), 7.46 – 7.36 (m, 1H), 7.31 – 7.21 (m, 2H), 7.17 (dd, J = 7.3, 1.3 Hz, 1H), 6.89 (d, J = 9.2 Hz, 1H), 6.80 (dd, J = 9.2, 2.4 Hz, 1H), 6.73 (d, J = 2.4 Hz, 1H), 6.14 (d, J = 14.0 Hz, 1H), 4.17 (q, J = 7.2 Hz, 2H), 3.63 – 3.52 (m, 4H), 2.68 (dd, J = 12.7, 6.7 Hz, 2H), 2.51 – 2.31 (m, 2H), 1.79 (d, J = 1.1 Hz, 6H), 1.41 (t, J = 7.2 Hz, 3H), 1.26 (t, J = 7.1 Hz, 6H). ^{13}C NMR (101 MHz, CD_3OD) δ = 171.78, 171.51, 163.49, 156.14, 155.75, 152.21,142.02, 140.91, 140.83, 137.64, 134.23, 129.93, 129.77, 128.82, 128.63, 178.43, 128.35, 124.42, 122.13, 120.90, 115.45, 113.94, 112.28, 110.01, 97.74, 95.11, 53.50, 48.86, 46.20, 44.81, 38.70, 27.58, 26.61, 24.04, 20.56, 11.60, 11.04, 7.93. MALDI-TOF MS for $C_{38}H_{41}N_2O_3^+$ = 573.1883.

Synthesis of FUC-1: Compound ND-1 (286 mg, 0.5 mmol) was dissolved in 10 mL CH_2Cl_2 and stirred vigorously at room temperature.

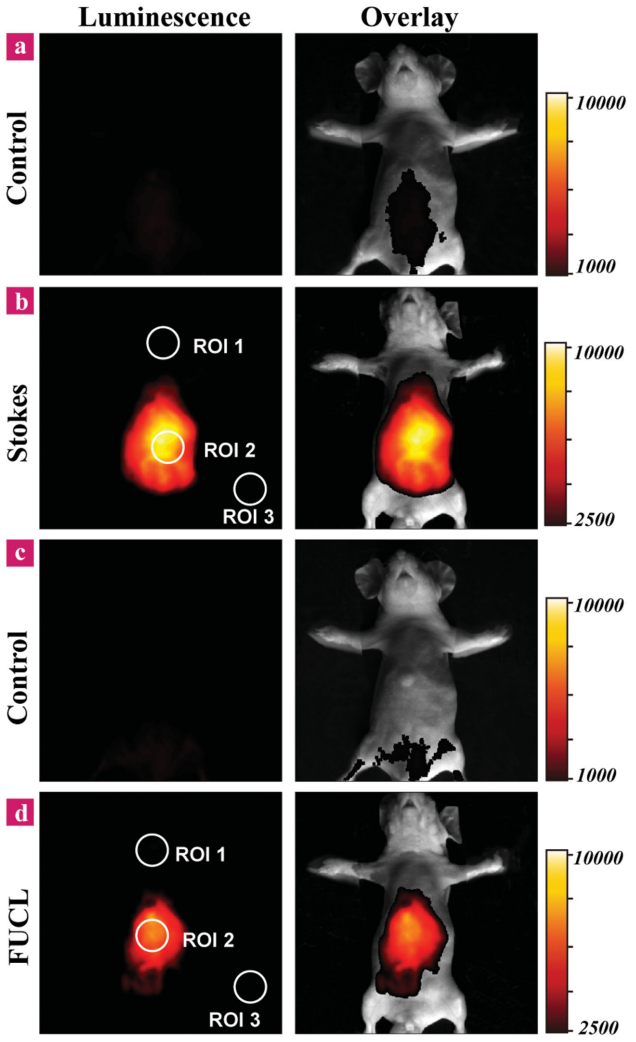

Figure 5. In vivo luminescence imaging of living mice. a) The luminescence image and the overlay image of the mouse injected with 0.2 mL normal saline and 0.2 mL FUC-1 (50 μM). b) The luminescence image and the overlay image of the 0.17 mg kg^{-1} wt $MeHg^+$-pretreatment living mouse injected with 0.2 mL FUC-1 (50 μM). c) The FUCL image and the overlay image of the mouse injected with 0.2 mL normal saline and 0.2 mL FUC-1 (50 μM). d) The FUCL image and the overlay image of the 0.17 mg kg^{-1} wt $MeHg^+$-pretreatment living mouse injected with 0.2 mL FUC-1 (50 μM). The luminescence and FUCL emission were all collected at 695–770 nm as detection signals, upon irradiation at 670 and 808 nm lasers, respectively.

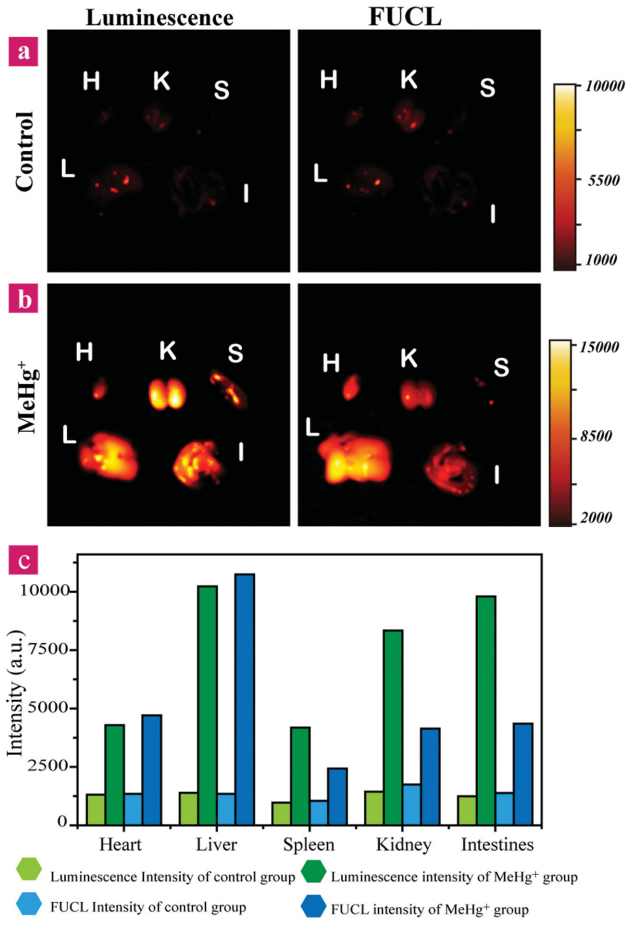

Figure 6. Ex vivo imaging of living mice. a) The luminescence and FUCL images of the control group: the mouse injected with 0.2 mL normal saline and 0.2 mL FUC-1 (50 μM). b) The luminescence and FUCL images of the $MeHg^+$ group: 0.17 mg kg^{-1} wt $MeHg^+$-pretreatment living mouse injected with 0.2 mL FUC-1 (50 μM). H: Heart; K: Kidney; S: Spleen; L: Liver; and I: Intestines. c) Luminescence and FUCL intensity analysis ex vivo.

Then phosphorus oxychloride (0.2 mL) was added dropwise in 5 min. The mixture was refluxed for 2 h. After cooling down, crude rhodamine acid chloride was obtained under vacuum. The crude product was dissolved in 10 mL THF, and 2 mL of saturated Na_2S aqueous solution was added. Then the mixture was stirred for 12 h at room temperature. After extracted with ethyl acetate, the extraction product was purified with silica chromatography using petroleum/ethyl acetate as eluent to obtain the yellow solid products. Yield 141 mg (48%). ^{1}H NMR (400 MHz, CD_3CN) δ = 7.93 (d, J = 7.8 Hz, 1H), 7.80 (t, J = 7.5 Hz, 1H), 7.68 (t, J = 7.5 Hz, 1H), 7.61 (t, J = 10.2 Hz, 1H), 7.44 (t, J = 14.1 Hz, 1H), 7.35 (dd, J = 13.2, 7.4 Hz, 1H), 7.31 (dd, J = 15.1, 7.5 Hz, 1H), 6.97 (t, J = 7.4 Hz, 1H), 6.83 (d, J = 7.8 Hz, 1H), 6.69 (d, J = 8.7 Hz, 1H), 6.56 – 6.46 (m, 2H), 5.63 (d, J = 12.6 Hz, 1H), 4.21 (q, J = 7.1 Hz, 1H), 3.85 (q, J = 7.1 Hz, 2H), 3.51 (q, J = 7.0 Hz, 4H), 2.82 – 2.54 (m, 2H), 2.27 (m, 2H), 1.81 (d, J = 1.6 Hz, 6H), 1.35 (t, J = 12.8 Hz, 3H), 1.29 – 1.25 (m, 6H). ^{13}C NMR (101 MHz, $CDCl_3$) δ = 156.22, 151.96, 148.38, 146.75, 144.38, 138.93, 136.36, 134.06, 129.71, 128.87, 127.66, 126.60, 122.60, 121.54, 119.80, 119.71, 119.22, 108.57, 107.84, 105.63, 104.93, 97.47, 91.62, 60.52, 44.35, 36.66, 31.86, 29.62, 28.28, 28.10, 25.27, 24.49,22.618, 22.35, 20.90, 14.03, 12.43, 10.86. MALDI-TOF MS for $C_{38}H_{41}N_2O_3^+$ = 588.2987.

Characterization of Photophysical Property: UV–vis absorption spectra were recorded on a Shimadzu 3000 spectrophotometer. Stokes luminescence spectra were measured on an Edinburgh FL920 luminescence spectrometer. The frequency upconversion luminescence spectra were also measured on the Edinburgh FL920 luminescence spectrometer, collecting with an 808 nm laser as light source. A 775 nm short-pass filter (semrock, Bright line FF01-775/SP-50 filter) was used between the sample and the detector. The absolute quantum yields of Stokes luminescence and anti-Stokes luminescence was measured by steady state/lifetime fluorescence spectrometer, collecting with a 60 mm integrating sphere (QM 40, Photo Technology International, Inc.).

Cell Culture and Laser Scan Luminescence Microscopy Imaging In Vitro: The cell lines Hela were provided by the Institute of Biochemistry and Cell Biology, SIBS, CAS (China). The Hela cells were grown in modified Eagles medium supplemented with 10% fetal bovine serum at 37 °C and 5% CO_2. The laser-scanning luminescence microscopy bioimaging

was performed with an OLYMPUS FV 1000 scanning unit collecting with lasers at 635 and 808 nm as the excitation source. Both the Stokes emission and the anti-Stokes emission were collected at 700–760 nm. Experiment to assess $MeHg^+$ uptake was performed over 0.5 h in the same medium supplemented with various concentration of $MeHg^+$. Before the experiments, Hela cells were washed with PBS buffer for at least three times to remove the excess $MeHg^+$, and then the cells were incubated with FUC-1 (10 μM) in PBS for 0.5 h at 37 °C. Cell imaging was then carried out after washing with PBS buffer.

Luminescence Bioimaging of Mercury In vivo. Animal procedures were in agreement with the guidelines of the institutional Animal Care and Use Committee. The Stokes luminescence bioimaging and anti-Stokes luminescence bioimaging were performed with a modified luminescence in vivo imaging system designed by our group. Two external adjustable lasers at 670 and 808 nm and an Andor DU897 EMCCD were used as the excitation source and the signal collector, respectively. The luminescence signals were collected at 695–770 nm with a 775 nm short-pass filter (Semrock).

Supporting Information

Supporting Information is available from the Wiley Online Library or from the author.

Acknowledgements

The authors thank State Key Basic Research Program of China (2013CB733700, 2015CB931800), National Science Foundation of China (51473078, 21231004, 21375024), Scientific and Technological Innovation Teams of Colleges and Universities in Jiangsu Province (TJ215006), Natural Science Foundation of Jiangsu Province (BM2012010), Synergetic Innovation Center for Organic Electronics and Information Displays, and Priority Academic Program Development of Jiangsu Higher Education Institutions (YX03001) for financial support.

Received: October 20, 2015
Revised: December 24, 2015
Published online: February 8, 2016

[1] a) N. S. Bloom, *Can. J. Fish. Aquat. Sci.* **1992**, *49*, 1010; b) D. W. Boening, *Chemosphere* **2000**, *40*, 1335; c) T. W. Clarkson, *Environ. Health Perspect.* **2002**, *110,* Suppl 1, 11.

[2] a) P. M. Bolger, B. A. Schwetz, *N. Engl. J. Med.* **2002**, *347*, 1735; b) T. W. Clarkson, *Crit. Rev. Clin. Lab. Sci.* **1997**, *34*, 369.

[3] a) E. M. Nolan, S. J. Lippard, *Chem. Rev.* **2008**, *108*, 3443; b) Y. Yang, Q. Zhao, W. Feng, F. Li, *Chem. Rev.* **2013**, *113*, 192.

[4] a) X. Q. Chen, S. W. Nam, M. J. Jou, Y. Kim, S. J. Kim, S. Park, J. Yoon, *Org. Lett.* **2008**, *10*, 5235; b) S. K. Ko, Y. K. Yang, J. Tae, I. Shin, *J. Am. Chem. Soc.* **2006**, *128*, 14150; c) J. V. Ros-Lis, M. D. Marcos, R. Martinez-Manez, K. Rurack, J. Soto, *Angew. Chem. Int. Ed. Engl.* **2005**, *44*, 4405; d) Y. K. Yang, K. J. Yook, J. Tae, *J. Am. Chem. Soc.* **2005**, *127*, 16760; e) S. Yoon, E. W. Miller, Q. He, P. H. Do, C. J. Chang, *Angew. Chem. Int. Ed. Engl.* **2007**, *46*, 6658; f) X. Zhang, Y. Xiao, X. Qian, *Angew. Chem. Int. Ed. Engl.* **2008**, *47*, 8025.

[5] a) E. Coronado, J. R. Galan-Mascaros, C. Marti-Gastaldo, E. Palomares, J. R. Durrant, R. Vilar, M. Gratzel, M. K. Nazeeruddin, *J. Am. Chem. Soc.* **2005**, *127*, 12351; b) L. Y. Cao, R. Zhang, W. Z. Zhang, Z. B. Du, C. J. Liu, Z. Q. Ye, B. Song, J. L. Yuan, *Biomaterials* **2015**, *68*, 21; c) Y. Liu, M. Li, Q. Zhao, H. Wu, K. Huang, F. Li, *Inorg. Chem.* **2011**, *50*, 5969.

[6] a) X. J. Xue, F. Wang, X. G. Liu, *J. Am. Chem. Soc.* **2008**, *130*, 3244; b) Q. Liu, J. Peng, L. Sun, F. Li, *ACS Nano* **2011**, *5*, 8040; c) D. Liu, S. Wang, M. Swierczewska, X. Huang, A. A. Bhirde, J. Sun, Z. Wang, M. Yang, X. Jiang, X. Chen, *ACS Nano* **2012**, *6*, 10999; d) J. S. Lee, M. S. Han, C. A. Mirkin, *Angew. Chem. Int. Ed. Engl.* **2007**, *46*, 4093.

[7] Z. Guo, W. Zhu, M. Zhu, X. Wu, H. Tian, *Chem. Eur. J.* **2010**, *16*, 14424.

[8] a) L. Yuan, W. Lin, K. Zheng, L. He, W. Huang, *Chem. Soc. Rev.* **2013**, *42*, 622; b) J. Zhou, Z. Liu, F. Li, *Chem. Soc. Rev.* **2012**, *41*, 1323.

[9] a) F. Auzel, *Chem. Rev.* **2004**, *104*, 139; b) G. Y. Chen, C. H. Yang, P. N. Prasad, *Acc. Chem. Res.* **2013**, *46*, 1474; c) G. S. He, L. S. Tan, Q. Zheng, P. N. Prasad, *Chem. Rev.* **2008**, *108*, 1245; d) H. M. Kim, B. R. Cho, *Chem. Rev.* **2015**, *115*, 5014; e) L. D. Sun, Y. F. Wang, C. H. Yan, *Acc. Chem. Res.* **2014**, *47*, 1001.

[10] a) S. K. Bae, C. H. Heo, D. J. Choi, D. Sen, E. H. Joe, B. R. Cho, H. M. Kim, *J. Am. Chem. Soc.* **2013**, *135*, 9915; b) R. Deng, X. Xie, M. Vendrell, Y.-T. Chang, X. Liu, *J. Am. Chem. Soc.* **2011**, *133*, 20168; c) H. M. Kim, B. R. Cho, *Acc. Chem. Res.* **2009**, *42*, 863; d) J. Liu, W. Bu, L. Pan, J. Shi, *Angew. Chem. Int. Ed. Engl.* **2013**, *52*, 4375; e) X. Xie, N. Gao, R. Deng, Q. Sun, Q. H. Xu, X. Liu, *J. Am. Chem. Soc.* **2013**, *135*, 12608.

[11] Y. Liu, M. Chen, T. Cao, Y. Sun, C. Li, Q. Liu, T. Yang, L. Yao, W. Feng, F. Li, *J. Am. Chem. Soc.* **2013**, *135*, 9869.

[12] a) M. H. Bartl, B. J. Scott, G. Wirnsberger, A. Popitsch, G. D. Stucky, *ChemPhysChem* **2003**, *4*, 392; b) J. L. Clark, G. Rumbles, *Phys. Rev. Lett.* **1996**, *76*, 2037.

[13] a) D. Bloor, G. Cross, P. K. Sharma, J. A. Elliott, G. Rumbles, *J. Chem. Soc. Faraday Trans.* **1993**, *89*, 4013; b) J. L. Clark, P. F. Miller, G. Rumbles, *J. Phys. Chem. A* **1998**, *102*, 4428; c) L. E. Erickson, *J. Lumin.* **1972**, *5*, 1; d) A. N. Kuzmin, A. Baev, A. V. Kachynski, T. S. Fisher, A. Shakouri, P. N. Prasad, *J. Appl. Phys.* **2011**,*110*, 033512; e) B. Stevens, *Chem. Rev.* **1957**, *57*, 439.

[14] a) R. K. Jain, T. k. Gustafso, S. S. Elliot, M. S. Chang, *J. Appl. Phys.* **1973**, *44*, 3157; b) A. V. Kachynski, A. N. Kuzmin, H. E. Pudavar, P. N. Prasad, *Appl. Phys. Lett.* **2005**, *87*, 023901; c) S. Kumazaki, *Chem. Phys.* **2013**, *419*, 107.

[15] L. Yuan, W. Lin, Y. Yang, H. Chen, *J. Am. Chem. Soc.* **2012**, *134*, 1200.

[16] X. Q. Zhan, Z. H. Qian, H. Zheng, B. Y. Su, Z. Lan, J. G. Xu, *Chem. Commun.* **2008**, 1859.

[17] a) W. Shi, H. M. Ma, *Chem. Commun.* **2008**, 1856; b) X. Chen, S. Q. Wu, J. H. Han, S. F. Han, *Bioorg. Med. Chem. Lett.* **2013**, *23*, 5295; c) H. Li, L. Y. Wang, *Analyst* **2013**, *138*, 1589.

[18] T. W. Clarkson, L. Magos, *Crit. Rev. Toxicol.* **2006**, *36*, 609.

[19] R. G. Pearson, *J. Am. Chem. Soc.* **1963**, *85*, 3533.

[20] a) P. Grandjean, P. J. Landrigan, *Lancet* **2006**, *368*, 2167; b) P. Grandjean, P. Weihe, R. F. White, F. Debes, S. Araki, K. Yokoyama, K. Murata, N. Sorensen, R. Dahl, P. J. Jorgensen, *Neurotoxicol. Teratol.* **1997**, *19*, 417.

[21] a) P. B. Tchounwou, W. K. Ayensu, N. Ninashvili, D. Sutton, *Environ. Toxicol.* **2003**, *18*, 149; b) F. Zahir, S. J. Rizwi, S. K. Haq, R. H. Khan, *Environ. Toxicol. Pharmacol.* **2005**, *20*, 351.